

Physical-biogeochemical interactions and potential effects on phytoplankton and *Ulva prolifera* in the coastal waters off Qingdao (Yellow Sea, China)

Qinsheng Wei^{1, 2, 3*}, Baodong Wang^{1, 2}, Qingzhen Yao^{2, 3}, Zhigang Yu^{2, 3}, Mingzhu Fu^{1, 2}, Junchuan Sun¹, Bochao Xu^{2, 3}, Linping Xie¹, Ming Xin¹

¹First Institute of Oceanography, Ministry of Natural Resources, Qingdao 266061, China

²Laboratory for Marine Ecology and Environmental Science, Pilot National Laboratory for Marine Science and Technology (Qingdao), Qingdao 266237, China

³Key Laboratory of Marine Chemistry Theory and Technology of Ministry of Education, Ocean University of China, Qingdao 266100, China

Received 2 July 2017; accepted 8 August 2018

© Chinese Society for Oceanography and Springer-Verlag GmbH Germany, part of Springer Nature 2019

Abstract

In recent years, the spectacular massive green tide of *Ulva prolifera* has become a recurrent phenomenon appearing every summer in the coastal waters off Qingdao (Yellow Sea, China), attracting the attention of scientists and local government. Based on multidisciplinary data collected during summer and winter, this study focuses on the hydrological characteristics and regional biogeochemical processes in coastal waters off Qingdao. The results show that the boundary of the Yellow Sea Cold Water Mass (YSCWM) can reach the Qingdao coastal region in summer and is locally raised to the upper layers to form coastal upwelling beyond tidal mixing and favorable wind. The regional summer upwelling off the Qingdao coast effectively enriches the nutrient concentrations in the upper water column and thus promotes growth of phytoplankton but reduces the dissolved oxygen (DO) concentration and pH value in the bottom. The regional summer upwelling off Qingdao coast may facilitate the growth and regional blooming of the *U. prolifera* that migrate to this region with the southerly wind. Additionally, the effects of the front on the aggregation of *U. prolifera* may be significant. In winter, the Yellow Sea Warm Current (YSWC) extends and spreads along the offshore region off the Subei Shoal towards the Qingdao coastal sea. This tongue-shaped warm water meets the cold coastal water off Qingdao, which leads to the formation of a physical front. As a consequence, remarkable fronts of nutrient and chlorophyll *a* (Chl *a*) also form between the shoreward warm water and the cold coastal water. This study increases the understanding of the interactions between the regional physical, chemical, and biological processes off the Qingdao coast.

Key words: biogeochemical process, upwelling, front, *Ulva prolifera*, Qingdao coast, southern Yellow Sea

Citation: Wei Qinsheng, Wang Baodong, Yao Qingzhen, Yu Zhigang, Fu Mingzhu, Sun Junchuan, Xu Bochao, Xie Linping, Xin Ming. 2019. Physical-biogeochemical interactions and potential effects on phytoplankton and *Ulva prolifera* in the coastal waters off Qingdao (Yellow Sea, China). Acta Oceanologica Sinica, 38(2): 11–23, doi: 10.1007/s13131-019-1344-3

1 Introduction

The South Yellow Sea (SYS) is a semi-enclosed epicontinental sea in the Northwest Pacific that is surrounded by the Shandong Peninsula, northern Jiangsu Province, and the Korean Peninsula. This region has specific topographic, hydrologic, chemical, and ecological characteristics (Tang and Su, 2000; Fu et al., 2009; Hwang et al., 2014; Lie and Cho, 2016; Wei, 2016; Wei et al., 2016a). Moreover, the SYS is significantly controlled by the East Asian monsoon climate, which includes prevailing northerly winds in winter and southerly winds in summer. The coastal area in the SYS contains significant variations in the sea-floor topography and complexity in the structure of the current field. Due to the impact of the Yellow Sea Warm Current (YSWC) (Teague

and Jacobs, 2000; Lie et al., 2009; Yu et al., 2010; Lin et al., 2011) in winter, and the Yellow Sea Cold Water Mass (YSCWM) (He et al., 1959; Yu et al., 2006; Zhang et al., 2008; Wang et al., 2014) at the bottom in summer, a remarkable front can form in the confluence region of the coastal water and the offshore water (Chen, 2009).

The Qingdao coastal region is located in the northwestern part of the SYS, where the coastline is generally oriented southwest-northeast. This region is deeper and has steeper topography than the other coastal areas of the western SYS (such as the Subei Shoal). The region of the SYS with depths >20 m can extend into this area (Fig. 1c), which may lead to differences in the dynamic characteristics and ecological responses between the Qingdao

Foundation item: The Open Fund of Laboratory for Marine Ecology and Environmental Science, Qingdao National Laboratory for Marine Science and Technology under contract No. LMEES201808; the Scientific and Technological Innovation Project of the Qingdao National Laboratory for Marine Science and Technology under contract No. 2016ASKJ02; the National Key Research and Development Program of China under contract Nos 2016YFC1402101 and 2017YFC1404402; the National Natural Science Foundation of China under contract No. 41606040; the National Project of Comprehensive Investigation and Research of Coastal Seas in China under contract No. 908-01-ST03.

*Corresponding author, E-mail: weiqinsheng@fio.org.cn

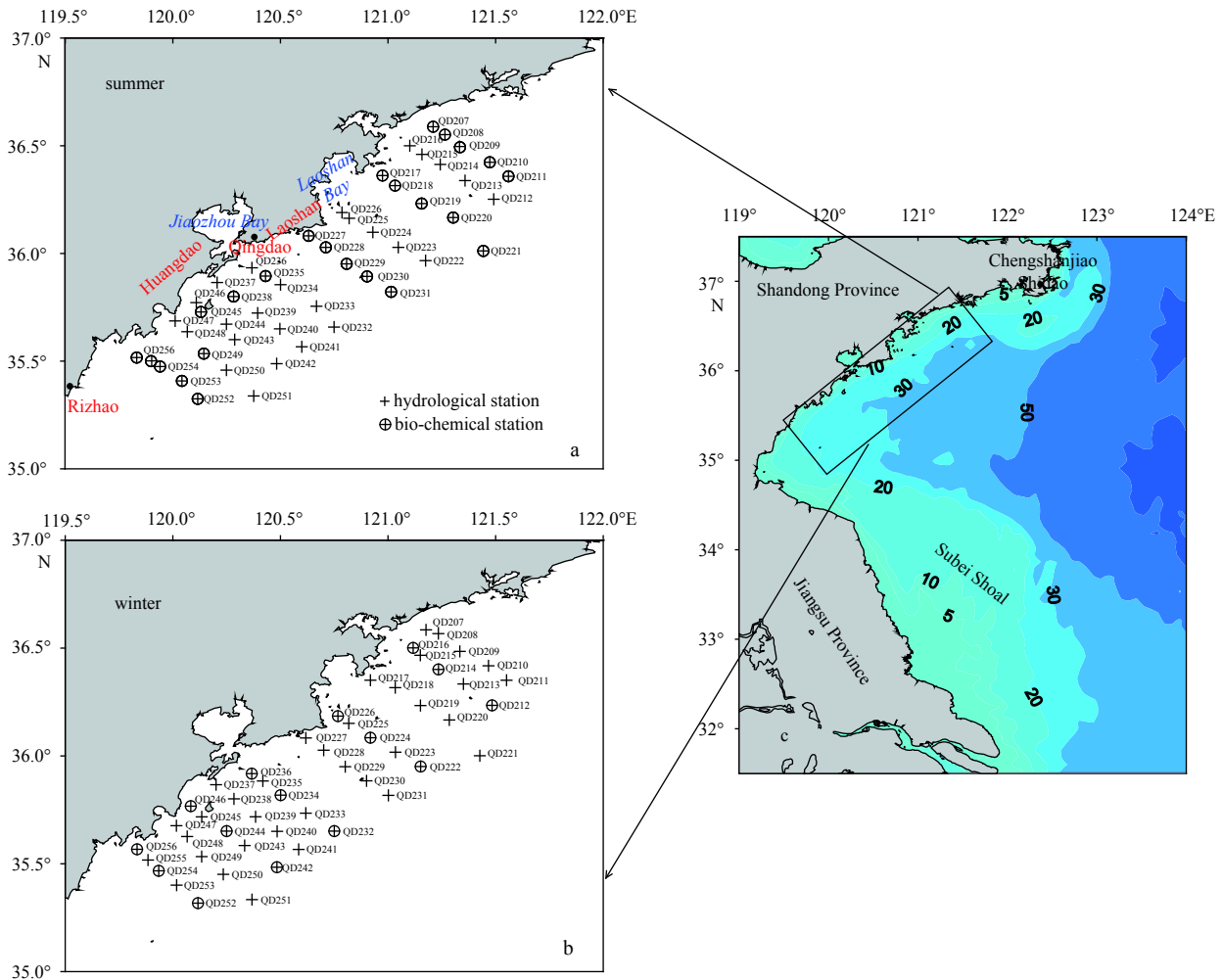


Fig. 1. Map of the study area showing the site locations off the Qingdao coast (a, b) and the topography with depth (m) isobaths (c) of the SYS. The black frame in Panel c indicates the study area.

coastal sea and the other coastal regions of the SYS. The large-scale bloom of green tide (*Ulva prolifera*) occurring in the SYS in 2008 and its aggregation off the Qingdao coast have drawn wide attention (Qiao et al., 2008; Liu et al., 2009). The green tide covered approximately 13 000–30 000 km² off the coast in the summer of 2008, posing a significant threat to the Olympic sailing events (Leliaert et al., 2009; Liu et al., 2009). In recent years, the recurrent *U. prolifera* in the Yellow Sea and its accumulation to the Qingdao coast in summer have not been negligible (Hu et al., 2010; Liu et al., 2010, 2013; Xu et al., 2014; Zhou et al., 2015; Qi et al., 2016), and the mean growth rate of *U. prolifera* can range from 10% to 20% per day in the coastal waters of Qingdao (Zhou et al., 2015). Additionally, the western SYS to the south of the Shandong Peninsula is an important spawning area for anchovies (Gao et al., 2003; Wan et al., 2008) and is also a district of concentrated human activities and economic development, including areas of intensive fish-farming (Sun et al., 1990; Xin et al., 2001). Besides, harmful algal blooms can occur in waters off the Qingdao coast as well (Yuan et al., 2017b). In this context, studying the physical-biogeochemical coupling off the Qingdao coast will increase the understanding of the regional ecological characteristics and provide scientific foundation for ecological research and management systems.

Previous studies have found that during summer, the tidal

front is prominent beyond the Subei Shoal and Chengshanjiao-Shidao near the boundary of the YSCWM (Zhao, 1985; Qi and Su, 1998; Ren et al., 2014), which can cause tide-induced frontal upwelling (Zhao, 1987; Lü et al., 2010; Yuan et al., 2017a; Wei et al., 2018). Furthermore, previous studies have noted that the tide-induced upwelling system beyond the Subei Shoal during summer can provide nutrients for the growth of *U. prolifera* while it drifts across the surface of the SYS (Qiao et al., 2011; Wei et al., 2018), and the nutrient contributions of the upwelling off the shoal is evaluated (Wei et al., 2018). As shown by studies of the physical processes off the Qingdao coast, the distribution of sunken *U. prolifera* in this region is closely in correspondence with the convergence and divergence of the current field, and the locations of the convergence and divergence correspond the high and low quantities of sunken *U. prolifera*, respectively (Lü and Qiao, 2008); the wind-driven sea surface current field and its annual variations are the main forcing dynamics for the accumulation of *U. prolifera* off the Qingdao coast and the changes in its drifting path (Qiao et al., 2011). Nevertheless, the physical-biogeochemical interactions and ecological impacts off the Qingdao coast remain poorly understood. Based on an analysis of the hydrological characteristics off the Qingdao coast with intensive station investigation, this study demonstrates that both the summer low-temperature, high-salinity YSCWM and the winter high-temper-

ature, high-salinity YSWC can extend to this region with a prominent front around its boundary. Therefore, we question the possibility of frontal upwelling off the Qingdao coast, where the boundary of the YSCWM can reach in summer. If so, how will it affect the regional biogeochemical processes and the aggregation of *U. prolifera*? In addition, the effects of the westward shift of the winter YSWC during its northward movement and its intrusion into the area to the south of the Shandong Peninsula (Su, 1986; Huang et al., 2005; Zhao et al., 2011) on the regional biogeochemical processes off the Qingdao coast cannot be ignored. Previously, by compiling the data collected in the entire western SYS, we studied the hydrological and chemical characteristics along the typical east-west (longitudinal) oriented cross-shelf transect (35°N), and the upwelling of cold water at the boundary of the YSCWM and its effect on vertical nutrient transport (Wei et al., 2016b). However, the hydrological characteristics off the Qingdao coast and the responses of the regional biogeochemical processes were not involved. Based on ship-board observations with intensive sampling and satellite-derived sea-surface temperature (SST) data, this study mainly analyzes the regional hydro-biogeochemical characteristics off the Qingdao coast as well as its ecological effects on the growth of phytoplankton chlorophyll *a* (Chl *a*) and *U. prolifera* to examine the physical-biogeochemical interactions in this region, interpreting the mechanisms that control the massive green tide occurrence off the Qingdao coast.

2 Materials and methods

This study is mainly based on the intensive sampling data acquired from the summer and winter cruises in the western SYS, which were conducted on board R/V *Beidou* in the region of 32°20'–36°40'N and west of 124°00'E, as previously shown by Wei et al. (2010a, b) and Fu et al. (2009); because this study focuses on the physical-biogeochemical coupling off the Qingdao coast, ten transects covering the Qingdao coastal region were selected. The summer investigation off the Qingdao coast was conducted from 14 to 16 July 2006, while the winter cruise was from 8 to 10 January, 2007; the station locations are shown in Fig. 1.

Hydrological parameters (temperature, salinity and density) of seawater were measured with a Sea-Bird 917 CTD (Sea-Bird Electronics, Bellevue, WA, USA). Water samples were collected with Niskin bottles attached to the CTD rosette at different depths (surface, 10 m and bottom) at each station for measurements of nitrate (NO₃-N), nitrite (NO₂-N), ammonia (NH₄-N), phosphate (PO₄-P), dissolved oxygen (DO), pH and Chl *a*. Water samples of nutrients were analyzed by spectrophotometry after filtration through cellulose acetate fiber filters (which were pre-treated by soaking in 1% (v/v) HCl for 24 h, washed by Mill-Q water until they were neutral, and burned at ~50°C for ~5 h). NO₃-N and NO₂-N were determined by the standard pink azo dye method and NH₄-N by the hypobromate oxidation-pink azo dye method; PO₄-P was determined by the standard molybdenum blue method. All of the methods and procedures were in accordance with those recommended by Parsons et al. (1984) and calibrated with standard substances (state second level standard substances of China). Dissolved inorganic nitrogen (DIN) was calculated as the total of NO₃-N, NO₂-N and NH₄-N. Samples for Chl *a* were filtered through GF/F filters and then frozen quickly at -20°C in the dark until analysis in the laboratory; Chl *a* was extracted in 90% (v/v) acetone and measured using a Turner Designs TD-700 fluorometer (Parsons et al., 1984).

In this study, the SST data were obtained from the National Oceanic and Atmospheric Administration's (NOAA's) National Climatic Data Center (<http://www.ncdc.noaa.gov/oisst/data-access>).

3 Results

The ranges and mean values of the physical and biogeochemical parameters in the coastal waters off Qingdao (Figs 1a, b) are summarized in Table 1. The temperatures in summer were generally much higher than those in winter, and the salinities in summer were slightly lower than in winter. For the biochemical parameters, the nutrient concentrations in summer were much lower than in winter, while the Chl *a* concentrations in summer were higher. The spatiotemporal distributions of the physical-biogeochemical parameters and their characteristics are described below.

Table 1. Statistic characteristics of the physical and biogeochemical parameters in the coastal waters off Qingdao

		Summer					Winter				
		<i>T</i> /°C	<i>S</i>	DIN/ μmol·L ⁻¹	PO ₄ -P/ μmol·L ⁻¹	Chl <i>a</i> / μg·L ⁻¹	<i>T</i> /°C	<i>S</i>	DIN/ μmol·L ⁻¹	PO ₄ -P/ μmol·L ⁻¹	Chl <i>a</i> / μg·L ⁻¹
Surface	Range	19.35–25.79	30.20–31.00	0.25–3.57	0.00–0.42	0.35–3.32	3.18–9.81	31.21–31.79	3.08–11.76	0.06–0.85	0.75–1.60
	Mean±SD	24.36±1.19	30.71±0.15	1.22±0.73	0.14±0.11	1.27±0.82	7.41±1.36	31.57±0.14	6.90±3.30	0.33±0.24	1.04±0.30
10 m	Range	11.12–25.12	30.50–31.88	0.66–5.12	0.00–0.36	0.48–6.31	2.98–9.82	31.23–31.80	3.40–11.73	0.10–0.67	0.81–1.72
	Mean±SD	20.90±3.76	30.96±0.31	1.52±1.07	0.16±0.12	1.70±1.28	7.36±1.43	31.57±0.13	6.43±3.08	0.32±0.18	1.11±0.31
Bottom	Range	8.43–25.17	30.19–31.59	0.53–4.49	0.00–0.38	0.49–2.21	2.98–9.82	31.24–31.79	3.20–12.06	0.08–0.71	-
	Mean±SD	16.14±5.14	31.07±0.32	1.77±1.03	0.18±0.11	1.23±0.47	7.34±1.44	31.57±0.13	6.82±3.61	0.34±0.21	-

3.1 Hydrological characteristics off the Qingdao coast

Figure 2 shows the horizontal distributions of the temperature, salinity, and density off the Qingdao coast in summer. As shown in Figs 2a–c, a region with surface temperatures below 24°C was present from southern area off the Jiaozhou Bay mouth to outside Laoshan Bay, which forms a cold core (19.35°C) at Sta. QD226 near the shore. Another small area with temperatures below 24°C was located off the Huangdao District. The surface salinity was high outside Laoshan Bay and off the Huangdao District. The surface density distribution was similar to the surface temperature distribution and contained high-density zones that corresponded to the low-temperature regions. At the 10 m layer

(Figs 2d–f), three notable low-temperature, high-salinity, and high-density areas were present in this region; one extended out from the Laoshan Bay, and the other two were located at the southeastern and southwestern parts of the study area. Moreover, the fronts around the low-temperature, high-salinity, and high-density areas were significant, and the temperature gradient magnitude seemed to reach the thresholds of 2.8°C and 1.4°C per 100 km, following Castelao and Wang (2014). At the bottom (Figs 2g–i), the temperature showed a clear onshore-offshore decreasing trend. In contrast, the salinity and density increased gradually from onshore to offshore. The low-temperature, high-salinity and high-density offshore waters tended to in-

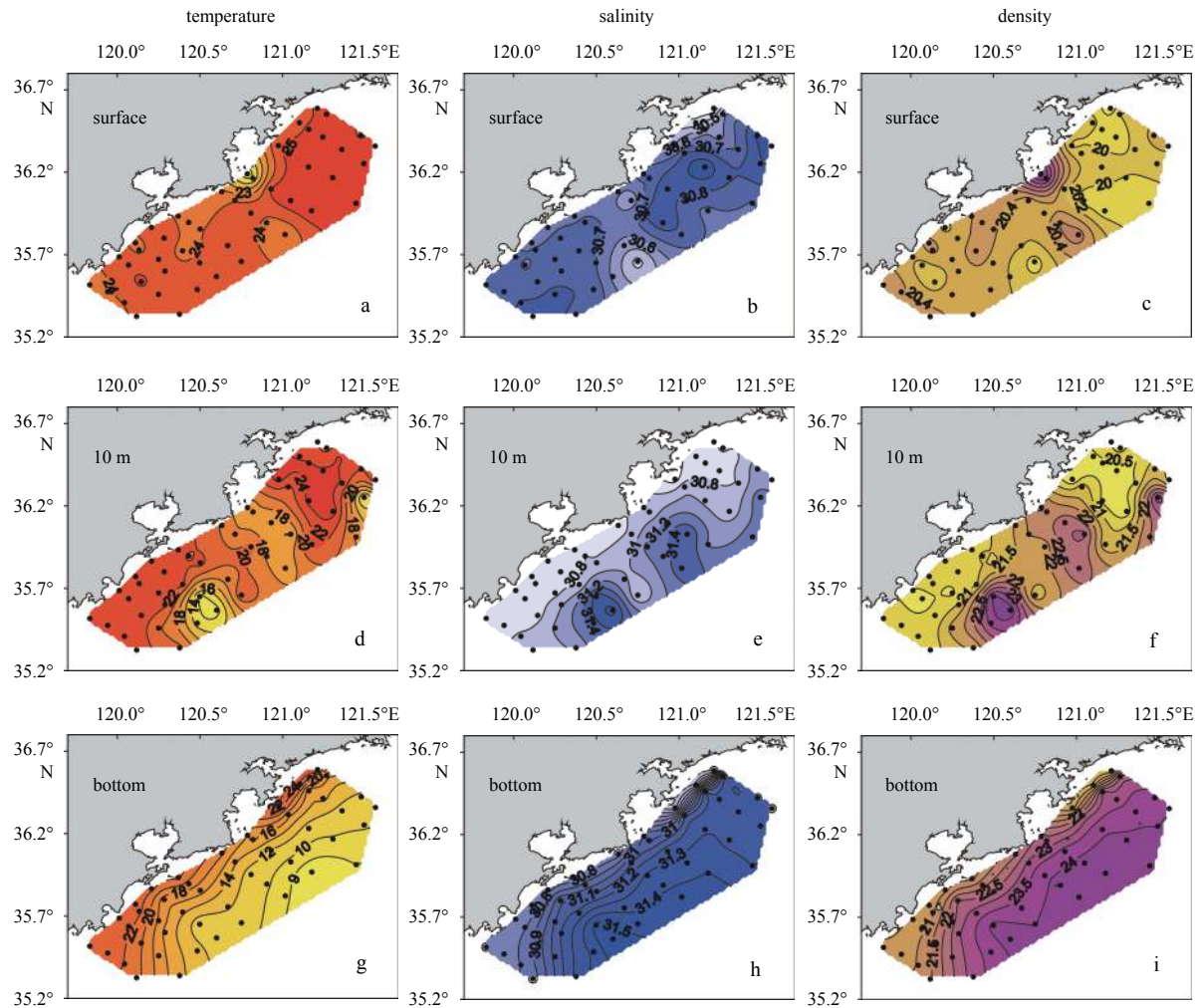


Fig. 2. Horizontal distributions of temperature ($^{\circ}\text{C}$), salinity, and density (kg/m^3) off the Qingdao coast in summer.

trude into the coastal region, and the cold water mass with temperatures below 16°C reached the southwestern part of the Laoshan Bay.

To reflect the vertical hydrological structure off the Qingdao coast during summer, Fig. 3 presents the vertical distributions of temperature and density along four typical transects. The vertical profiles of the hydrological parameters along each transect displayed a three-layer structure. The upper mixed layer, which can be determined using a quasi-step function approximation method (Ge et al., 2003), was generally warmer than 20°C and had a low density. Below the upper mixed layer, a strong thermocline and pycnocline were present at a depth of ~ 10 m. Within the thermocline and pycnocline, the water temperature decreased rapidly, whereas the density increased rapidly. Under the thermocline, a relatively homogenous bottom water with low-temperature and high-density was present. The temperature and density contours along transects tended to be uplifted significantly at the steep slopes near the shores; the 20°C isothermal line near the shore along Transect QD226–QD222 reached the surface (Fig. 3b).

Figure 4 shows the horizontal distributions of the temperature, salinity, and density off the Qingdao coast during winter. As shown in Figs 4a and b, the surface temperature and salinity varied from low near the shore to high offshore. The minimum temperature was located in the northwestern part of the study area.

The hydrological contours were generally parallel to the coast and showed significant gradients, as indicated by the significantly positive linear relationship between temperature and station depth ($R^2=0.66$, $p<0.01$). The high-temperature and high-salinity offshore water reached the coastal region to the Jiaozhou Bay mouth and the area to the south of Laoshan, which indicated the intrusion of the offshore water into the Qingdao coastal region. Corresponding to the shoreward extension of the warm water, the cold water off the Qingdao coast extended outward near the areas outside the Huangdao region, southeast of the mouth of Jiaozhou Bay, and southeast of the mouth of Laoshan Bay. The density distribution generally varied from high near the shore to low offshore and formed a high-density zone that corresponded to the region of low temperatures in the northeastern part of the study area (Fig. 4c). The distributions and values of temperature, salinity, and density at the bottom (Figs 4d–f) were similar to those at the surface. Notably, the water column was well mixed vertically in winter; thus, the vertical distributions of the temperature, salinity, and density in winter are not shown.

3.2 Biochemical characteristics off the Qingdao coast

Figure 5 shows the horizontal distributions of nutrients and Chl-*a* off the Qingdao coast in summer. From the surface to the bottom, the concentrations of $\text{PO}_4\text{-P}$ and DIN both varied from high near the shore ($\text{PO}_4\text{-P}>0.2$ $\mu\text{mol}/\text{L}$, $\text{DIN}>1.6$ $\mu\text{mol}/\text{L}$) to low off-

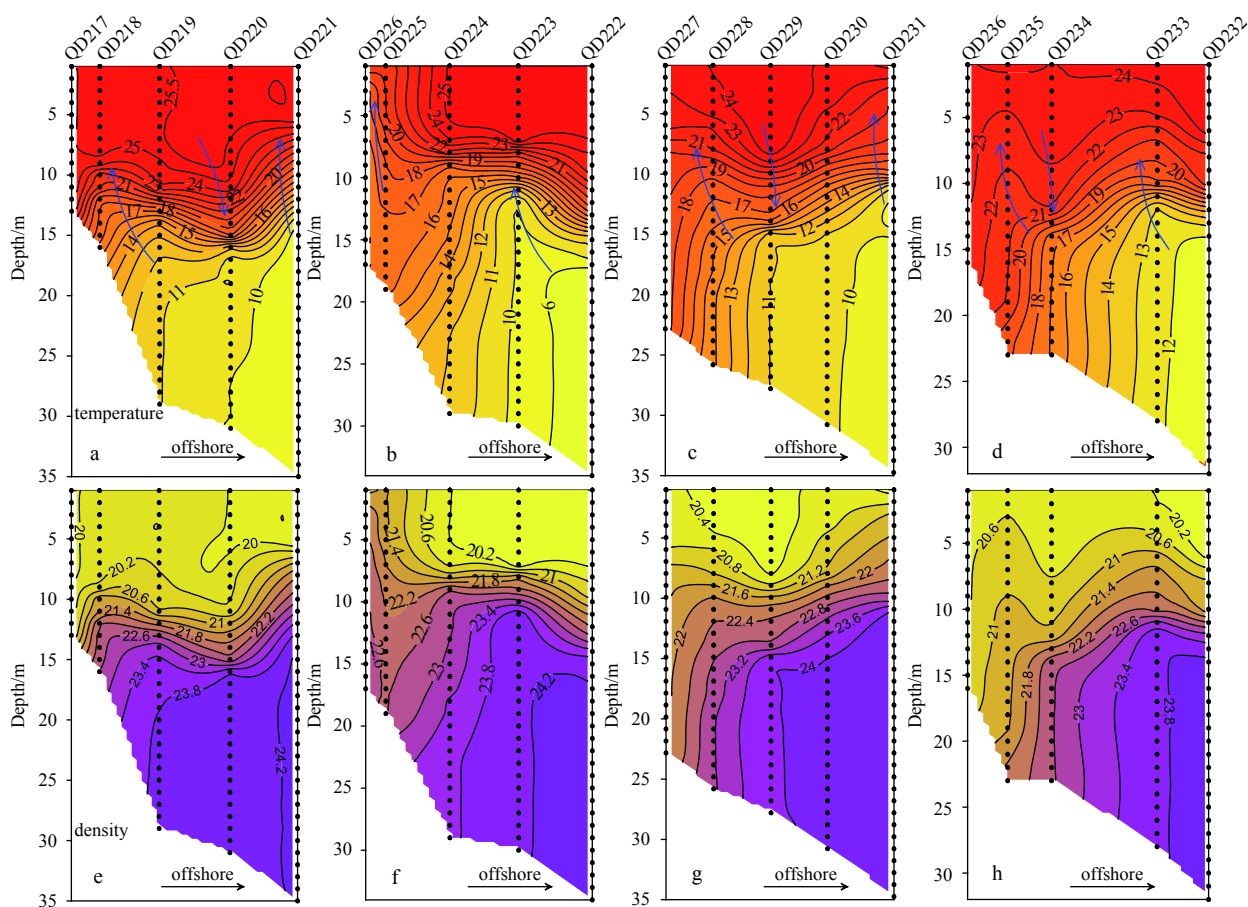


Fig. 3. Vertical distributions of temperature ($^{\circ}\text{C}$) and density (kg/m^3) along typical transects off the Qingdao coast in summer. The arrows in Panels a–d indicate the tide-induced upwelled or downwelled waters.

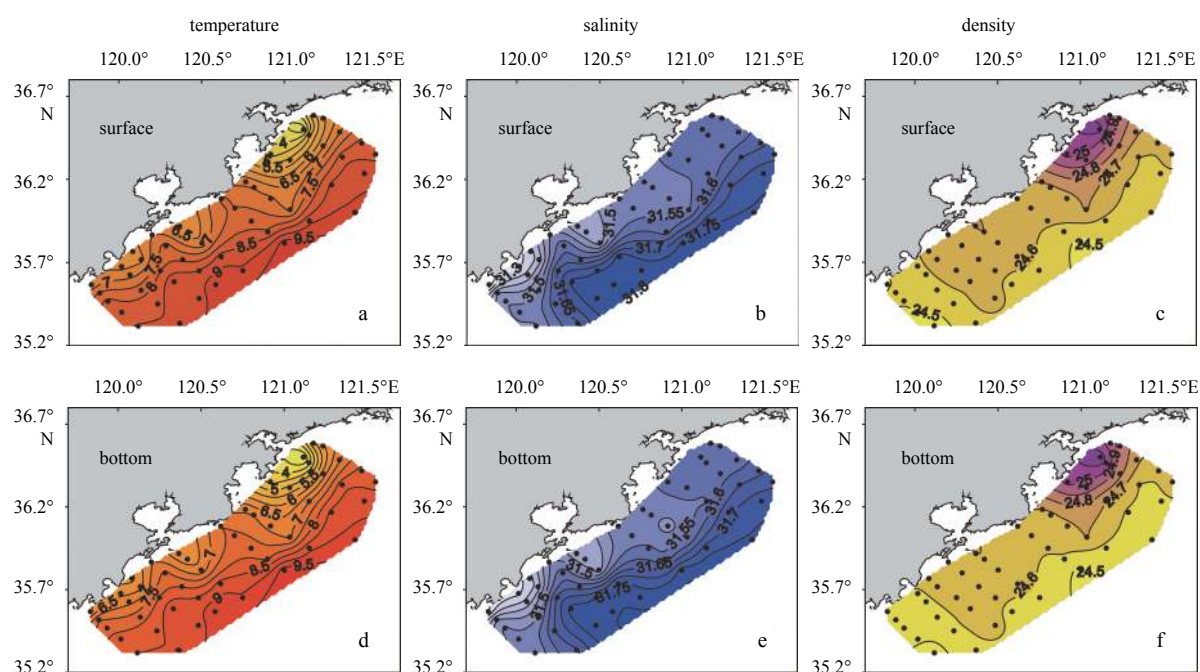


Fig. 4. Horizontal distributions of temperature ($^{\circ}\text{C}$), salinity, and density (kg/m^3) off the Qingdao coast in winter.

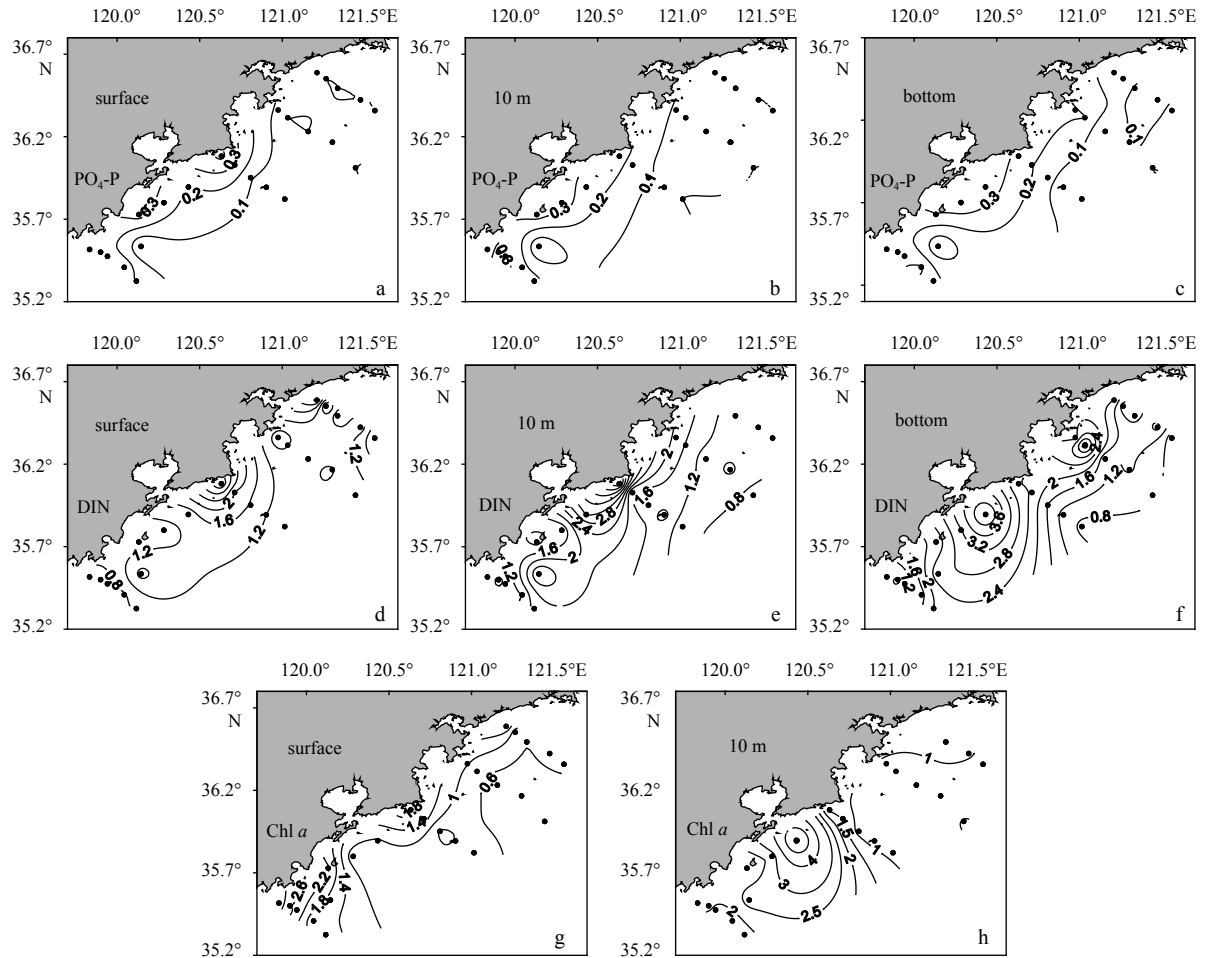


Fig. 5. Horizontal distributions of nutrients ($\mu\text{mol/L}$) and Chl *a* ($\mu\text{g/L}$) off the Qingdao coast in summer.

shore ($\text{PO}_4\text{-P} < 0.2 \mu\text{mol/L}$, $\text{DIN} < 1.6 \mu\text{mol/L}$) (Figs 5a–f). Furthermore, a high-value core ($\text{PO}_4\text{-P} = 0.42 \mu\text{mol/L}$, $\text{DIN} = 3.57 \mu\text{mol/L}$) of surface nutrients was located to the south of Laoshan (Figs 5a, d). The distribution of Chl *a* at the surface was similar to that of the nutrients, showing a decreasing trend from onshore ($> 1.0 \mu\text{g/L}$) to offshore ($< 1.0 \mu\text{g/L}$) (Fig. 5g). At the 10 m layer, an area of high Chl *a* concentrations ($> 4.0 \mu\text{g/L}$) was located southeast of the mouth of Jiaozhou Bay (Fig. 5h).

Figure 6 shows the vertical distributions of the relevant biochemical parameters off the Qingdao coast in summer. The concentrations of nutrients and Chl *a* were higher near the shore than offshore, whereas the DO and pH had opposite distributions. Further analysis shows that both the nearshore high-nutrient ($\text{NO}_3\text{-N} > 1.0 \mu\text{mol/L}$), high-Chl *a* ($> 1.0 \mu\text{g/L}$) zones and the low-DO ($< 6.0 \text{mg/L}$), low-pH (< 8.0) areas along Transect QD217–QD221 were found at the steep slope near the shore, which was in agreement with the uplifting locations of the high-density, low-temperature water (Fig. 3) in this region. Similar phenomena were also observed along Transect QD227–QD231.

shows the horizontal distributions of nutrients and Chl *a* off the Qingdao coast in winter. Although the concentrations of nutrients in this region in winter are significantly higher than those in summer (Figs 5a–f), the overall distribution patterns were generally identical. From the surface to the bottom, the concentrations decreased gradually from nearshore to offshore, and the contours were generally parallel to the coastline (Figs 7a–f). At

the surface and the 10-m layers, the Chl *a* concentrations varied from low near the shore ($< 1.0 \mu\text{g/L}$) to high offshore ($> 1.0 \mu\text{g/L}$) (Figs 7g, h).

4 Discussion

4.1 Upwelling and onshore intrusion of the offshore water to the Qingdao coast

Based on the water masses and current structure in the SYS (Yu et al., 2006; Zhang et al., 2008; Lin et al., 2011; Wei et al., 2016b), we can conclude that the summer offshore cold bottom water off the Qingdao coast was affected by YSCWM, whereas the winter high-temperature, high-salinity water that extended to the Qingdao coast was influenced by the YSWC.

Previous studies have shown that significant tide-induced upwelling occurs beyond the Subei Shoal and the Chengshanjiao-Shidao at the boundary of the YSCWM, which leads to the formation of surface cold water (Xia and Guo, 1983; Zhao, 1987; Lü et al., 2010; Wei et al., 2018). The distribution of the averaged SST from satellite remote sensing in the western SYS during the summer investigation period (Fig. 8a) shows this phenomenon clearly. Through an in-depth analysis of the regional hydrological characteristics off the Qingdao coast, our results indicate that the boundary of the Yellow Sea summer cold water mass could reach the Qingdao coast and was locally raised to the upper layer to form coastal upwelling. The surface low-temperature zone

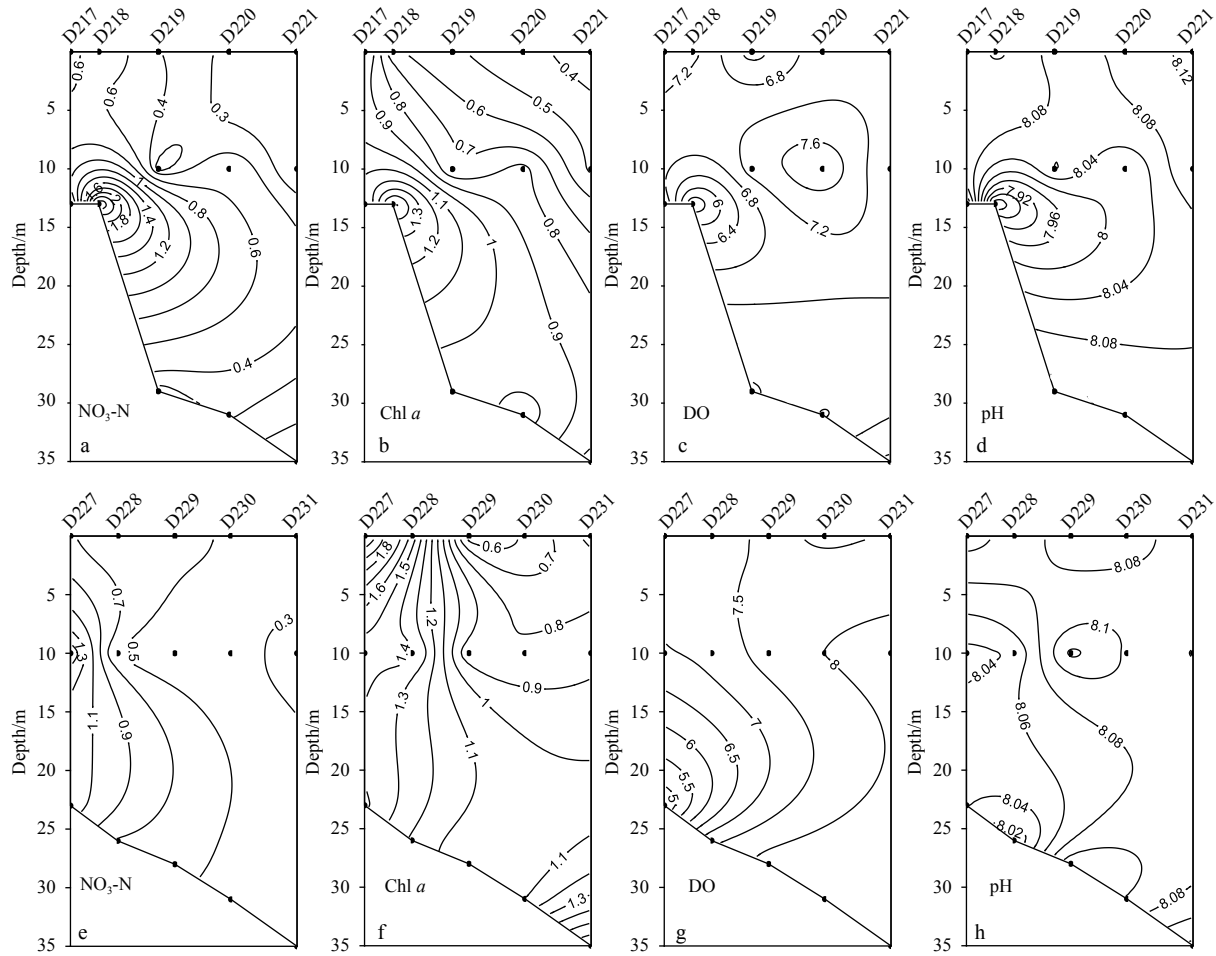


Fig. 6. Vertical distributions of $\text{NO}_3\text{-N}$ ($\mu\text{mol/L}$), $\text{Chl } a$ ($\mu\text{g/L}$), DO (mg/L), and pH off the Qingdao coast in summer.

(<24°C) from the southern area off the mouth of Jiaozhou Bay to outside Laoshan Bay and that off the Huangdao District (Fig. 2a) were both caused by the upwelling of the bottom YSCWM, which also resulted in corresponding high-density zones (Fig. 2c). The surface temperature-salinity scatter plot (Fig. 9a) can further confirm the upwelling off the Qingdao coast. These findings indeed reveal the existence of upwelling in this coast area, as implied by Bao et al. (2017) and Yuan et al. (2017a). It should be noted that the upwelling of the nearshore water may lead to the sinking of the outer edge of the coastal water under the control of mass conservation, which further induces the rising of seawater far from the shore to some extent. This can be observed in the vertical distributions of the hydrological parameters (Fig. 3). In particular, significant upwelling occurred near Sta. QD218 on Transect QD217–QD221, Sta. QD228 on Transect QD227–QD231, and Sta. QD235 on Transect QD236–QD232. While Stas QD220, QD229 and QD234, which are located outside the aforementioned upwelling stations, experienced downwelling. Meanwhile, the seawater rose slightly near the offshore Stas QD221, QD231 and QD233. Therefore, near the 10 m layer, seawater temperature varied from low to high to low from nearshore to offshore (Figs 3a–d). This pattern illustrates the seaward transition of upwelling to downwelling to upwelling off the Qingdao coast. Notably, the scope of upwelling off the Qingdao coast was generally smaller and closer to the coast than the upwelling that occurred beyond the Subei Shoal and Chengshanjiao–Shidao, and the surface low-temperature water due to the upwelling was also slightly

warmer (Fig. 8a). This result shows the spatial difference of upwelling at the boundary of the YSCWM in summer.

Coastal upwelling usually occurs when the subsurface waters move upward to compensate the offshore movement of surface waters. Generally speaking, the causes of upwelling mainly include wind forcing, topography, tidal mixing, stratification, and background flow (Hu and Wang, 2016). As indicated by previous studies, the upwelling and surface cold water near the boundary of the YSCWM in the Yellow Sea in summer is mainly induced by tidal mixing beyond proper topography (Zhao, 1987; Qi and Su, 1998; Lü et al., 2010), and the southerly wind can enhance the upwelling off the western coasts of the Yellow Sea (Lü et al., 2010; Bao et al., 2017). Considering that the boundary area of the YSCWM can reach the coast area of Qingdao, it is reasonable that the tidal mixing plays a role in the upwelling formation off the Qingdao coast by stirring the bottom water upward (Lü et al., 2010). Moreover, a southwesterly/southerly alongshore wind is dominant in the coast area of Qingdao, when the southwest Asian monsoon prevails in boreal summer. This wind stress can drive the surface water to move offshore (the right of the wind direction) in the northern hemisphere due to the Ekman transport effect (Ekman, 1905) and lead to the consequent divergence off the coast, which permits the drawing up of the bottom water to maintain mass conservation; as a result, the upwelling and SST cooling are triggered. In addition, the intensified upwelling-favorable wind can also induce an increase in frontal probabilities, with SST fronts and alongshore wind stress significantly correl-

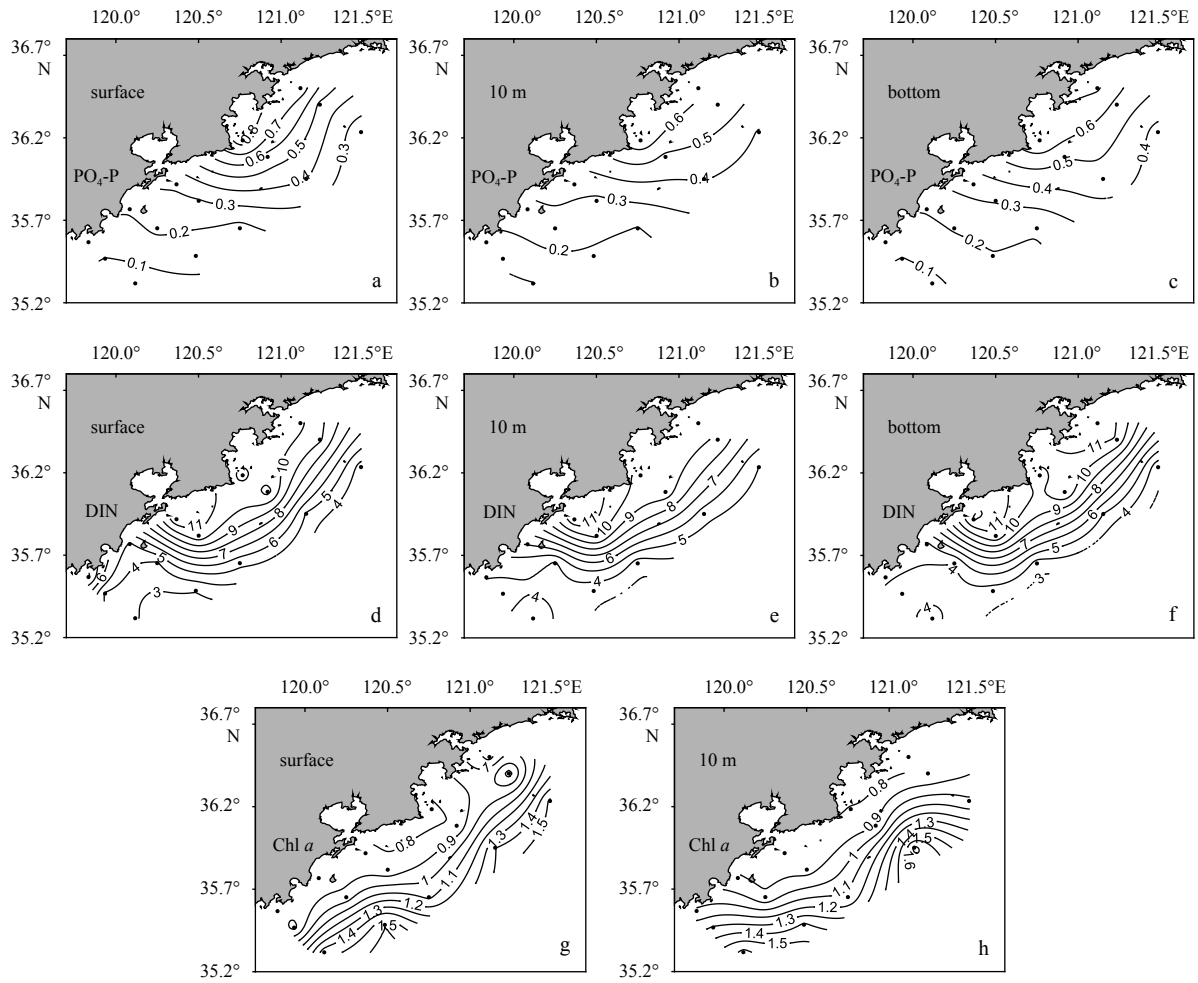


Fig. 7. Horizontal distributions of nutrients ($\mu\text{mol/L}$) and *Chl a* ($\mu\text{g/L}$) off the Qingdao coast in winter.

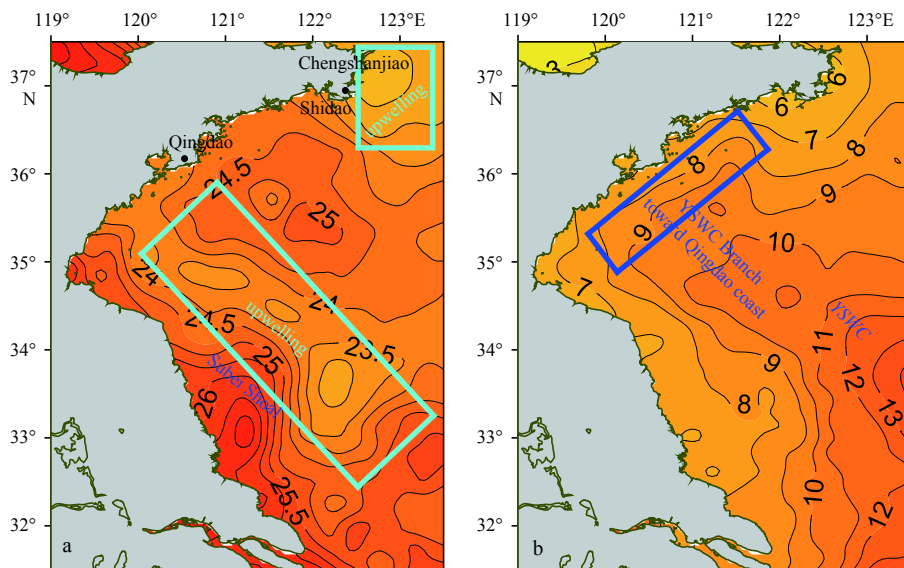


Fig. 8. Distributions of the averaged SST ($^{\circ}\text{C}$) in the SYS from satellite remote sensing during the investigation period. a. July 14–16, 2006 and b. January 8–10, 2007. The light blue boxes in Panel a indicate the upwelling areas with temperature below 23.5°C , whereas the dark blue box in Panel b shows the front of northwestern branch of the YSWC.

ated (Wang et al., 2015). Based on aforementioned analyses, a schematic view demonstrating the mechanisms of the upwelling

in the coast of Qingdao is further provided in Fig. 10a. In general, the upwelling with relatively low SST and frontal activities off the

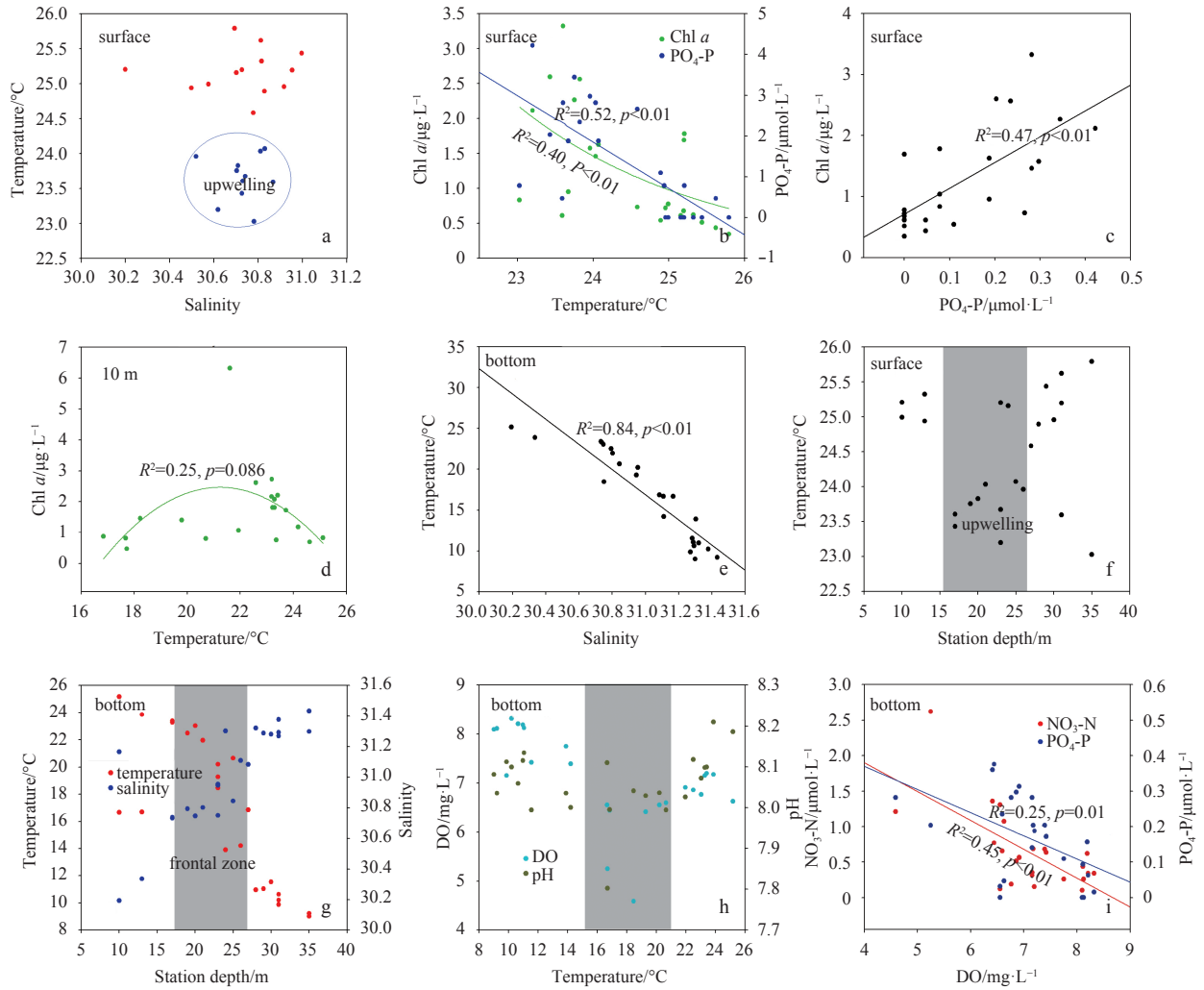


Fig. 9. Correlations between the physical-biochemical parameters off the Qingdao coast in summer. The gray area in Panel h indicates the bottom temperature frontal zone where the low DO and pH occurred.

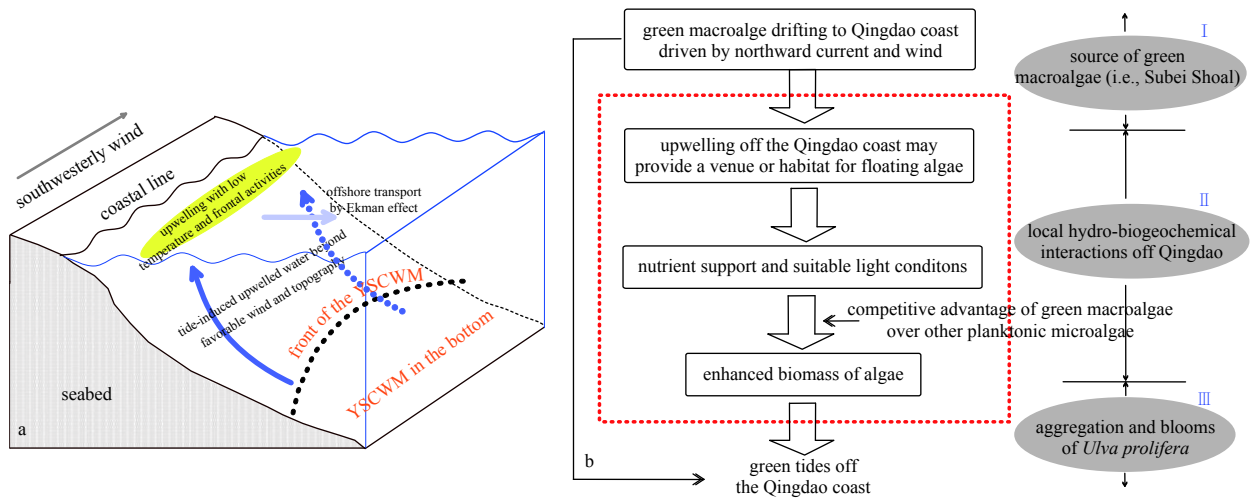


Fig. 10. Conceptual diagram demonstrating the upwelling (a) and schematic chart (b) illustrating the development of green tides off the Qingdao coast.

Qingdao coast is the combined effects of tide mixing and wind stress. Notably, induced by tidal mixing, a cross-frontal secondary circulation can be formed around the boundary of the

YSCWM; bottom waters ascend along the slope and flow back together with the original surface waters (Lü et al., 2010). Consequently, the waters in the upper layer on the offshore side of

the upwelling are forced down. This mechanism can illustrate the seaward transition of upwelling to downwelling off the Qingdao coast (Figs 3a–d).

In winter, the YSWC brings high-temperature, high-salinity water into the SYS, which plays a critical role in the mass exchange between the SYS and the East China Sea (Guo et al., 2003; Yuan et al., 2008). Furthermore, the physical processes associated with the YSWC can influence the nutrient distribution (Liu et al., 2015; Wei et al., 2016b), phytoplankton (Fu et al., 2009; Liu et al., 2015) and zooplankton (Wang et al., 2003; Wang and Zuo, 2004; Lü et al., 2013) biomass, anchovy migration (Wei et al., 2016a), and also community structure (Wang and Zuo, 2004; Liu et al., 2015), highlighting the complexity of ecosystem dynamics in the SYS. Previous studies have shown that during the northward intrusion of the YSWC from the southeastern SYS, its path can change to some extent (Su, 1986; Huang et al., 2005; Zhao et al., 2011). It usually forms a branch toward the Shandong Peninsula near 35°N (Su, 1986). As clearly shown in the distribution of the averaged SST from satellite remote sensing in the western SYS during the winter investigation period (Fig. 8b), the tongue-shape warm water of the YSWC extended along the offshore region off the Subei Shoal toward the region south of the Shandong Peninsula and converged with the nearshore cold water off the Qingdao coast. The temperature and salinity off the Qingdao coast were affected by the interaction between the high-salinity offshore warm water that intruded onshore and the seaward low-salinity cold water (Fig. 4). Additionally, our results also show that corresponding to the shoreward expansion of the warm water from southwest of the mouth of Jiaozhou Bay and south of Laoshan, the cold water off the Qingdao coast extended seaward from outside Huangdao District, southeast of the mouth of Jiaozhou Bay, and southeast of the mouth of Laoshan Bay (Figs 4a, d), which led to the opposing cross-like water exchange between the offshore warm water and the nearshore cold water off the Qingdao coast.

4.2 Regional biogeochemical responses to the physical processes off the Qingdao coast

The area to the south of the Shandong Peninsula, which has high transparency and moderate temperature and salinity, is ideal for the habitat, growth, and reproduction of marine organisms (Tang and Su, 2000; Gao et al., 2003). To analyze the biogeochemical responses to the hydrological characteristics off the Qingdao coast in summer, the correlations between the physical-biochemical parameters are shown in Fig. 9. As illustrated in Figs 9b and c, the surface $\text{PO}_4\text{-P}$ (other main nutrients were distributed similarly and thus are not shown) and Chl *a* off the Qingdao coast were negatively correlated with temperature in summer; the high-nutrient and high-Chl *a* stations were mainly located in regions with temperatures below 24°C; the Chl *a* and $\text{PO}_4\text{-P}$ presented a positive correlation. This indicates that the upwelling region off the Qingdao coast could provide nutrients for the growth of phytoplankton; thus, the high-Chl *a* area and the coastal upwelling region were correlated. Moreover, the high-nutrient region to the south of Laoshan (Figs 5a, d) was at least partially caused by the coastal upwelling, which could also be implied by the uprising of the nearshore high-nutrient water along Transect QD227–QD231 (Fig. 6e). At the 10-m layer (Fig. 9d), the Chl *a* concentrations were high at the frontal zone (21.5–23.5°C) adjacent to the low-temperature cold water (<21°C, Fig. 2d). The deviation in the locations of the high-Chl *a* and the low-temperature stations may be related to the relatively low temperature in the central upwelling region. In addition, a phytoplankton patch with

high Chl *a* was observed near the bottom at Sta. QD218 (Fig. 6b). This phenomenon may be related with the subsurface convergence effect due to the upward moving of bottom layer waters in upwelling area; in this case, the phytoplankton sinking from the upper layers can be assembled and thus contributes the patch of high Chl *a*.

Statistical analysis also shows that the bottom temperature and salinity off the Qingdao coast were well correlated in summer (Fig. 9e). The surface low-temperature upwelling region was mainly concentrated at station depths ranging from 15 to 26 m (Fig. 9f); the regions with significant gradients (i.e., frontal zone) in the bottom temperature and salinity were also generally located in this range of water depths (Fig. 9g). Additionally, the stations with low DO and pH at the bottom corresponded to temperatures of approximately 15–21°C (Fig. 9h). This temperature range corresponded to the bottom frontal zone (Fig. 9g). The aforementioned results show that the upwelling and the bottom frontal zones off the Qingdao coast were generally located at the steep slope with depths of 15–26 m and corresponded to low DO and pH at the bottom. The formation of the low DO and pH at the bottom was related to oxygen consumption by the decomposition of organic matter, and this process was also accompanied by the release of nutrients. The above biochemical behavior is indicated by the negative correlation between the nutrients and DO at the bottom (Fig. 9i). Consequently, we suggest that the nutrients transported vertically by the upwelling off the Qingdao coast in summer originated partially from regeneration during the decomposition of the local organic matter. Undoubtedly, induced by the upwelling off the Qingdao coast, the in-situ nutrients at the bottom can be brought to the surface and therefore play an important role in maintaining the relatively high concentrations of Chl *a* in the upper layers.

As shown in the relationships between the physical-biochemical parameters off the Qingdao coast in winter, the temperature and salinity presented a significant positive correlation (Fig. 11a), and the concentrations of Chl *a* at the surface and 10 m layers were both positively correlated with temperature (Fig. 11b). In the nearshore area, more intensive vertical mixing and low temperature may be not beneficial to the growth of phytoplankton, being responsible for the low phytoplankton biomass. While, due to the drifting property and aggregation of phytoplankton, the high-Chl *a* region could appear in the frontal zone formed by the intersection of the tongue-shaped YSWC and the coastal water in the SYS, as indicated by Wei et al. (2016a). Moreover, the higher temperature in the offshore frontal zone may be also favorable for the stay of phytoplankton. This can explain the seaward increasing trend of Chl *a* concentration off the Qingdao coast in winter. Because the offshore diffusion and transport of nutrients from coast is limited, together with the phytoplankton consumption (especially in the offshore), the nutrient concentrations were generally low in the offshore high-temperature region off the Qingdao coast, which partially led to a negative correlation between nutrients and temperature (Fig. 11c). Subsequently, nutrient and Chl *a* fronts formed between the shoreward warm water and the coastal cold water (Fig. 7). This result illustrates the controlling effect of the winter hydrological characteristics off the Qingdao coast on the growth of phytoplankton in this region.

4.3 Potential effects of the physical-biogeochemical processes on the regional growth and aggregation of *Ulva prolifera* off the Qingdao coast

The large-scale blooms of *U. prolifera* have resulted in a major ecological disaster in the SYS over the past few years (Liu et

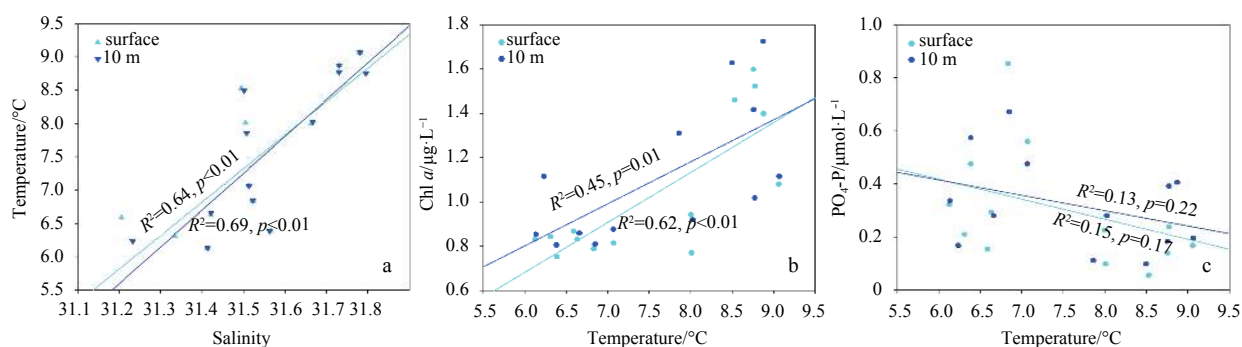


Fig. 11. Correlations between the physical-biochemical parameters off the Qingdao coast in the winter.

al., 2013; Zhou et al., 2015). Due to the sea surface current field, which is driven by the southerly monsoon in summer, the *U. prolifera* that originates from the Subei Shoal tends to drift northward (Qiao et al., 2011; Lee et al., 2011; Bao et al., 2015). During the northward drifting process, the frontal upwelling system beyond the Subei Shoal can provide nutrients for the growth of *U. prolifera* (Wei et al., 2018). Notably, *U. prolifera* shows a competitive advantage over other species during its various developmental stages (germling, seedling, and adult); once *U. prolifera* propagules germinate, they can exhibit strong inhibitory effects on the growth of planktonic microalgae in multiple ways, including allelopathy and nutrient competition (Liu, 2015). As a result, there is a negative correlation between the occurrence of *U. prolifera* and Chl *a* concentration in the SYS, as revealed by Sun et al. (2018). Consequently, based on the analyses presented in Sections 4.1 and 4.2, it is conclusive that the summer upwelling off the Qingdao coast may facilitate the growth of the *U. prolifera* (by providing nutrients in a unique venue) that drifts to this region from the Subei Shoal as well, further contributing to the regional propagation and bloom of *U. prolifera* during the period from early summer to July. Moreover, the upwelled waters can also exhibit much better light transmission, which is conducive to the growth of *U. prolifera* too, just like the case off the Subei Shoal (Wei et al., 2018). Accordingly, a schematic process-flow chart illustrating the development of green tides off the Qingdao coast is summarized in Fig. 10b. In addition, due to the regional upwelling and downwelling (Fig. 3), the radial convergence and divergence of *U. prolifera* off the Qingdao coastal sea may be significant. Driven by the stable southerlies in summer, the sunken *U. prolifera* can assemble in bands near the shore due to the effect of the southwest-northeast oriented bottom front (Figs 2g–i), as previously indicated by the *U. prolifera* distribution based on Moderate Resolution Imaging Spectroradiometer (MODIS) satellite images (see Fig. 3 in Qiao et al., 2011). The aforementioned understanding provides a viewpoint of *U. prolifera* blooms off the Qingdao coast, partially interpreting the marine environment-driven mechanisms for this cross-regional ecological disaster in the SYS.

5 Conclusions

Based on in-situ observations and satellite-derived SST data in summer and winter, the physical-biogeochemical interactions and potential effects on phytoplankton and *U. prolifera* off the Qingdao coast are investigated.

(1) Upwelling (summer) and onshore intrusion (winter) of the offshore water exist off the Qingdao coast. The boundary of the bottom YSCWM can reach the Qingdao coast and is locally raised to the upper waters to form coastal upwelling in summer beyond

tidal mixing and favorable wind. In winter, the YSWC extends and spreads beyond the Subei Shoal toward the region south of the Shandong Peninsula and converges with the nearshore cold water off the Qingdao coast.

(2) The hydrological characteristics off the Qingdao coast influence the local growth of phytoplankton significantly. The summer regional upwelling off the Qingdao coast provides an effective supplement of nutrients to the upper layers and thus promotes the growth of phytoplankton and leads to corresponding low DO and pH at the bottom front. Prominent fronts of nutrients and Chl *a* form between the shoreward warm water and the nearshore cold water in winter.

(3) The hydrological characteristics off the Qingdao coast during summer can potentially affect the regional reproduction and aggregation of *U. prolifera*. The regional upwelling off the Qingdao coast may facilitate the growth of *U. prolifera* that drifts to this region with the southerlies and thus cause regional *U. prolifera* blooms. The effect of the summer frontal activities off the Qingdao coast on the aggregation of *U. prolifera* cannot be ignored.

Our findings reveal that the upwelling and frontal activities off the Qingdao coast provide scenarios for local mesoscale processes. In future studies, physical-biogeochemical modeling and further exploration are needed to obtain an in-depth understanding about the role of upwelling in regional ecosystem. Specifically, nutrient enrichment experiments using the upwelled waters should be carried out to investigate and evaluate quantitatively the influence of upwelling on the growth of phytoplankton and *U. prolifera*.

Acknowledgments

We are grateful to the survey team and crew for their help and cooperation during the field investigation.

References

- Bao Min, Guan Weibing, Yang Yang, et al. 2015. Drifting trajectories of green algae in the western Yellow Sea during the spring and summer of 2012. *Estuarine, Coastal and Shelf Science*, 163: 9–16, doi: [10.1016/j.ecss.2015.02.009](https://doi.org/10.1016/j.ecss.2015.02.009)
- Bao Shaowu, Li Xiaofeng, Shen Dongliang, et al. 2017. Ocean upwelling along the Yellow Sea coast of China revealed by satellite observations and numerical simulation. *IEEE Transactions on Geoscience and Remote Sensing*, 55(1): 526–536, doi: [10.1109/TGRS.2016.2610761](https://doi.org/10.1109/TGRS.2016.2610761)
- Castelao R M, Wang Yuntao. 2014. Wind-driven variability in sea surface temperature front distribution in the California Current System. *Journal of Geophysical Research: Oceans*, 119(3): 1861–1875, doi: [10.1002/2013JC009531](https://doi.org/10.1002/2013JC009531)
- Chen C T A. 2009. Chemical and physical fronts in the Bohai, Yellow

- and East China seas. *Journal of Marine Systems*, 78(3): 394–410, doi: [10.1016/j.jmarsys.2008.11.016](https://doi.org/10.1016/j.jmarsys.2008.11.016)
- Ekman V W. 1905. On the influence of the earth's rotation on ocean-currents. *Arkiv för Matematik, Astronomi Och Fysik*, 2(11): 1–53
- Fu Mingzhu, Wang Zongling, Li Yan, et al. 2009. Phytoplankton biomass size structure and its regulation in the Southern Yellow Sea (China): Seasonal variability. *Continental Shelf Research*, 29(18): 2178–2194, doi: [10.1016/j.csr.2009.08.010](https://doi.org/10.1016/j.csr.2009.08.010)
- Gao Shengquan, Lin Yi'an, Jin Mingming, et al. 2003. Distribution of nutrient and its relationship with anchovy spawning ground in the southern waters of Shandong Peninsula. *Haiyang Xuebao (in Chinese)*, 25(Suppl 2): 157–166
- Ge Renfeng, Qiao Fangli, Yu Fei, et al. 2003. A method for calculating thermocline characteristic elements in shelf sea area—Quasi-step function approximation method. *Advances in Marine Science (in Chinese)*, 21(4): 393–400
- Guo Binghuo, Hu Xiaomin, Xiong Xuejun, et al. 2003. Study on interaction between the coastal water, shelf water and Kuroshio water in the Huanghai Sea and East China Sea. *Acta Oceanologica Sinica*, 22(3): 351–367
- He Chongben, Wang Yuanxiang, Lei Zongyou, et al. 1959. A preliminary study of the formation of Yellow Sea Cold Water Mass and its properties. *Oceanologia et Limnologia Sinica (in Chinese)*, 2(1): 11–15
- Hu Chuanmin, Li Daqiu, Chen Changsheng, et al. 2010. On the recurrent *Ulva prolifera* blooms in the Yellow Sea and East China Sea. *Journal of Geophysical Research*, 115: C05017
- Huang Daji, Fan Xiaopeng, Xu Dongfeng, et al. 2005. Westward shift of the Yellow Sea warm salty tongue. *Geophysical Research Letters*, 32: L24613, doi: [10.1029/2005GL024749](https://doi.org/10.1029/2005GL024749)
- Hu Jianyu, Wang Xiaohua. 2016. Progress on upwelling studies in the China seas. *Reviews of Geophysics*, 54: 653–673, doi: [10.1002/2015RG000505](https://doi.org/10.1002/2015RG000505)
- Hwang J H, Van Sy P, Choi B J, et al. 2014. The physical processes in the Yellow Sea. *Ocean & Coastal Management*, 102: 449–457
- Lee J H, Pang I C, Moon I J, et al. 2011. On physical factors that controlled the massive green tide occurrence along the southern coast of the Shandong Peninsula in 2008: A numerical study using a particle-tracking experiment. *Journal of Geophysical Research*, 116: C12036, doi: [10.1029/2011JC007512](https://doi.org/10.1029/2011JC007512)
- Leliaert F, Zhang Xiaowen, Ye Naihao, et al. 2009. Research note: Identity of the Qingdao algal bloom. *Phycological Research*, 57(2): 147–151, doi: [10.1111/pre.2009.57.issue-2](https://doi.org/10.1111/pre.2009.57.issue-2)
- Lie H J, Cho C H. 2016. Seasonal circulation patterns of the Yellow and East China Seas derived from satellite-tracked drifter trajectories and hydrographic observations. *Progress in Oceanography*, 146: 121–141, doi: [10.1016/j.pocean.2016.06.004](https://doi.org/10.1016/j.pocean.2016.06.004)
- Lie H J, Cho C H, Lee S. 2009. Tongue-shaped frontal structure and warm water intrusion in the southern Yellow Sea in winter. *Journal of Geophysical Research*, 114: C01003
- Lin Xiaopei, Yang Jiayan, Guo Jingsong, et al. 2011. An asymmetric upwind flow, Yellow Sea Warm Current: 1. New observations in the western Yellow Sea. *Journal of Geophysical Research*, 116: C04026
- Liu Qing. 2015. The interactions study between bloom-forming *Ulva prolifera* and phytoplankton in the Yellow Sea (in Chinese) [dissertation]. Qingdao: University of Chinese Academy of Sciences
- Liu Xin, Chiang K P, Liu Sumei, et al. 2015. Influence of the Yellow Sea Warm Current on phytoplankton community in the central Yellow Sea. *Deep Sea Research Part I: Oceanographic Research Papers*, 106: 17–29, doi: [10.1016/j.dsr.2015.09.008](https://doi.org/10.1016/j.dsr.2015.09.008)
- Liu Dongyan, Keesing J K, Dong Zhijun, et al. 2010. Recurrence of the world's largest green-tide in 2009 in Yellow Sea, China: *Porphyra yezoensis* aquaculture rafts confirmed as nursery for macroalgal blooms. *Marine Pollution Bulletin*, 60(9): 1423–1432, doi: [10.1016/j.marpolbul.2010.05.015](https://doi.org/10.1016/j.marpolbul.2010.05.015)
- Liu Dongyan, Keesing J K, He Peimin, et al. 2013. The world's largest macroalgal bloom in the Yellow Sea, China: formation and implications. *Estuarine, Coastal and Shelf Science*, 129: 2–10, doi: [10.1016/j.ecss.2013.05.021](https://doi.org/10.1016/j.ecss.2013.05.021)
- Liu Dongyan, Keesing J K, Xing Qianguo, et al. 2009. World's largest macroalgal bloom caused by expansion of seaweed aquaculture in China. *Marine Pollution Bulletin*, 58(6): 888–895, doi: [10.1016/j.marpolbul.2009.01.013](https://doi.org/10.1016/j.marpolbul.2009.01.013)
- Lü Xin'gang, Qiao Fangli. 2008. Distribution of sunken macroalgae against the background of tidal circulation in the coastal waters of Qingdao, China, in summer 2008. *Geophysical Research Letters*, 35: L23614, doi: [10.1029/2008GL036084](https://doi.org/10.1029/2008GL036084)
- Lü Xin'gang, Qiao Fangli, Xia Changshui, et al. 2010. Upwelling and surface cold patches in the Yellow Sea in summer: Effects of tidal mixing on the vertical circulation. *Continental Shelf Research*, 30(6): 620–632, doi: [10.1016/j.csr.2009.09.002](https://doi.org/10.1016/j.csr.2009.09.002)
- Lü Lian'gang, Wang Xiao, Wang Huiwu, et al. 2013. The variations of zooplankton biomass and their migration associated with the Yellow Sea Warm Current. *Continental Shelf Research*, 64: 10–19, doi: [10.1016/j.csr.2013.05.007](https://doi.org/10.1016/j.csr.2013.05.007)
- Parsons T R, Maita Y, Lalli C M. 1984. *A Manual of Chemical and Biological Methods for Seawater Analysis*. Oxford: Pergamon Press
- Qi Lin, Hu Chuanmin, Xing Qianguo, et al. 2016. Long-term trend of *Ulva prolifera* blooms in the western Yellow Sea. *Harmful Algae*, 58: 35–44, doi: [10.1016/j.hal.2016.07.004](https://doi.org/10.1016/j.hal.2016.07.004)
- Qi Jianhua, Su Yusong. 1998. Numerical simulation of the tide-induced continental front in the Yellow Sea. *Oceanologia et Limnologia Sinica (in Chinese)*, 29(3): 247–254
- Qiao Fangli, Ma Deyi, Zhu Mingyuan, et al. 2008. The green macroalgal bloom in the Yellow Sea in 2008 and the scientific countmeasures. *Advances in Marine Science (in Chinese)*, 26(3): 409–410
- Qiao Fangli, Wang Guansuo, Lü Xin'gang, et al. 2011. Drift characteristics of green macroalgae in the Yellow Sea in 2008 and 2010. *Chinese Science Bulletin*, 56(21): 2236–2242, doi: [10.1007/s11434-011-4551-7](https://doi.org/10.1007/s11434-011-4551-7)
- Ren Shihe, Xie Jiping, Zhu Jiang. 2014. The roles of different mechanisms related to the tide-induced fronts in the Yellow Sea in summer. *Advances in Atmospheric Sciences*, 31(5): 1079–1089, doi: [10.1007/s00376-014-3236-y](https://doi.org/10.1007/s00376-014-3236-y)
- Su Yusong. 1986. A survey of geographical environment, circulation systems and the central fishing grounds in the Huanghai Sea and East China Sea. *Journal of Shandong College of Oceanology (in Chinese)*, 16(1): 12–27
- Sun Xiao, Wu Mengquan, Xing Qianguo, et al. 2018. Spatio-temporal patterns of *Ulva prolifera* blooms and the corresponding influence on chlorophyll-a concentration in the Southern Yellow Sea, China. *Science of the Total Environment*, 640–641: 807–820
- Sun Yao, Yu Hong, Yang Qinfang, et al. 1990. Analysis and evaluation of nutritional condition and chemical indexes in Dingzi Bay waters. *Journal of Fisheries of China (in Chinese)*, 14(1): 33–39
- Tang Qisheng, Su Jilan. 2000. *Study on Ecosystem Dynamics in Chinese Coastal Ocean I: Key Scientific Question and Study Stratagem (in Chinese)*. Beijing: Science Press
- Teague W J, Jacobs G A. 2000. Current observations on the development of the Yellow Sea Warm Current. *Journal of Geophysical Research*, 105(C2): 3401–3411, doi: [10.1029/1999JC900301](https://doi.org/10.1029/1999JC900301)
- Wan Ruijing, Wei Hao, Sun Shan, et al. 2008. Spawning ecology of the anchovy *Engraulis japonicus* in the spawning ground of the Southern Shandong Peninsula I. Abundance and distribution characters of anchovy eggs and larvae. *Acta Zoologica Sinica (in Chinese)*, 54(5): 785–797
- Wang Yuntao, Castelao R M, Yuan Yeping. 2015. Seasonal variability of alongshore winds and sea surface temperature fronts in Eastern Boundary Current Systems. *Journal of Geophysical Research: Oceans*, 120(3): 2385–2400, doi: [10.1002/2014JC010379](https://doi.org/10.1002/2014JC010379)
- Wang Rong, Gao Shangwu, Wang Ke, et al. 2003. Zooplankton indication of the Yellow Sea Warm Current in winter. *Journal of Fisheries of China (in Chinese)*, 27(Suppl): 39–48
- Wang Bin, Hirose N, Kang B, et al. 2014. Seasonal migration of the Yellow Sea Bottom Cold Water. *Journal of Geophysical Research: Oceans*, 119(7): 4430–4443, doi: [10.1002/2014JC009873](https://doi.org/10.1002/2014JC009873)
- Wang Rong, Zuo Tao. 2004. The Yellow Sea Warm Current and the Yellow Sea Cold Bottom Water: their impact on the distribution of zooplankton in the southern Yellow Sea. *Journal of the Korean Society of Oceanography*, 39: 1–13

- Wei Qinsheng. 2016. Characteristics and mechanisms of chemical hydrology and ecological responses in the southern Yellow Sea and off the Changjiang Estuary (in Chinese) [dissertation]. Qingdao: Ocean University of China
- Wei Qinsheng, Li Xiansen, Wang Baodong, et al. 2016a. Seasonally chemical hydrology and ecological responses in frontal zone of the central southern Yellow Sea. *Journal of Sea Research*, 112: 1–12, doi: [10.1016/j.seares.2016.02.004](https://doi.org/10.1016/j.seares.2016.02.004)
- Wei Qinsheng, Liu Lu, Zhan Run, et al. 2010a. Distribution features of the chemical parameters in the Southern Yellow Sea in summer. *Periodical of Ocean University of China (in Chinese)*, 40(1): 82–88
- Wei Qinsheng, Wang Baodong, Yao Qingzhen, et al. 2018. Hydrobiogeochemical processes and their implications for *Ulva prolifera* blooms and expansion in the world's largest green tide occurrence region (Yellow Sea, China). *Science of the Total Environment*, 645: 257–266, doi: [10.1016/j.scitotenv.2018.07.067](https://doi.org/10.1016/j.scitotenv.2018.07.067)
- Wei Qinsheng, Yu Zhigang, Wang Baodong, et al. 2016b. Coupling of the spatial-temporal distributions of nutrients and physical conditions in the southern Yellow Sea. *Journal of Marine Systems*, 156: 30–45, doi: [10.1016/j.jmarsys.2015.12.001](https://doi.org/10.1016/j.jmarsys.2015.12.001)
- Wei Qinsheng, Zhou Ming, Wei Xiuhua, et al. 2010b. Distribution features and variation tendency of chemical elements in the southern Yellow Sea in winter. *Advances in Marine Science (in Chinese)*, 28(3): 353–363
- Xia Zongwan, Guo Binghuo. 1983. The cold water and upwelling in the tip areas of Shandong peninsula and Liaodong peninsula. *Journal of Oceanography of Huanghai & Bohai Seas (in Chinese)*, 1(1): 13–19
- Xin Fuyan, Qu Keming, Cui Yi, et al. 2001. Distribution and variation of dissolved nutrient inorganic nitrogen and phosphorous in Aoshan Bay. *Journal of Fishery Sciences of China (in Chinese)*, 8(4): 79–82
- Xu Qing, Zhang Hongyuan, Ju Lian, et al. 2014. Interannual variability of *Ulva prolifera* blooms in the Yellow Sea. *International Journal of Remote Sensing*, 35(11–12): 4099–4113
- Yu Fei, Zhang Zhixin, Diao Xinyuan, et al. 2006. Analysis of evolution of the Huanghai Sea Cold Water Mass and its relationship with adjacent water masses. *Haiyang Xuebao (in Chinese)*, 28(5): 26–34
- Yu Fei, Zhang Zhixin, Diao Xinyuan, et al. 2010. Observational evidence of the Yellow Sea Warm Current. *Chinese Journal of Oceanology and Limnology*, 28(3): 677–683, doi: [10.1007/s00343-010-0006-2](https://doi.org/10.1007/s00343-010-0006-2)
- Yuan Dongliang, Li Yao, Wang Bin, et al. 2017a. Coastal circulation in the southwestern Yellow Sea in the summers of 2008 and 2009. *Continental Shelf Research*, 143: 101–117, doi: [10.1016/j.csr.2017.01.022](https://doi.org/10.1016/j.csr.2017.01.022)
- Yuan Yongquan, Yu Zhiming, Song Xiuxian, et al. 2017b. Temporal and spatial characteristics of harmful algal blooms in Qingdao Waters, China. *Chinese Journal of Oceanology and Limnology*, 35(2): 400–414, doi: [10.1007/s00343-016-5279-7](https://doi.org/10.1007/s00343-016-5279-7)
- Yuan Dongliang, Zhu Jianrong, Li Chunyan, et al. 2008. Cross-shelf circulation in the Yellow and East China Seas indicated by MODIS satellite observations. *Journal of Marine Systems*, 70(1–2): 134–149
- Zhang Shuwen, Wang Qingye, Lü Yan, et al. 2008. Observation of the seasonal evolution of the Yellow Sea Cold Water Mass in 1996–1998. *Continental Shelf Research*, 28(3): 442–457, doi: [10.1016/j.csr.2007.10.002](https://doi.org/10.1016/j.csr.2007.10.002)
- Zhao Baoren. 1985. The fronts of the Huanghai Sea Cold Water Mass induced by tidal mixing. *Oceanologia et Limnologia Sinica (in Chinese)*, 16(6): 451–460
- Zhao Baoren. 1987. A preliminary study of continental shelf fronts in the western part of southern Huanghai Sea and circulation structure in the front region of the Huanghai Cold Water Mass (HCWM). *Oceanologia et Limnologia Sinica (in Chinese)*, 18(3): 217–226
- Zhao Sheng, Yu Fei, Diao Xinyuan, et al. 2011. The path and mechanism of the Yellow Sea Warm Current. *Marine Science (in Chinese)*, 35(11): 73–80
- Zhou Mingjiang, Liu Dongyan, Anderson D M, et al. 2015. Introduction to the special issue on green tides in the Yellow Sea. *Estuarine, Coastal and Shelf Science*, 163: 3–8, doi: [10.1016/j.ecss.2015.06.023](https://doi.org/10.1016/j.ecss.2015.06.023)